

## Sudden Impulse Environment for Cigre Technical Brochure

Edward B. Savage\* <sup>(1)</sup>, William A. Radasky<sup>(1)</sup>, and James L. Gilbert<sup>(1)</sup>  
 (1) Metatech Corporation. Goleta, California, 93119, <http://www.metatechcorp.com>

### Abstract

Cigre is in the process of producing a technical brochure on geomagnetic storm environments – this paper will summarize the sudden impulse environment term.

### 1. Introduction

Cigre Technical Brochure (TB) WG C4.32 “Understanding of the Geomagnetic Environment for the High Voltage Power Grid” will include the three geomagnetic environments:

1. Sudden Impulse
2. Auroral Electrojet
3. Coronal Hole

This paper will deal with the sudden impulse (SI) term. Initially its main purpose is to present a sampling of SI measurements from around the world, and under various conditions. The measured magnetic field disturbances will be converted to electric fields in the ground, which is what is of concern for electric power grids. Of special concern is possible variation with position, such as latitude, and misconceptions about what terms are needed to define the environment.

The original main emphasis of the TB was collection of SI measurements from stations spread out around the world, and conversion of these into electric fields. Originally there was a limited set of magnetometer stations used – limited to availability of fast cadence data. There was some 1-second data from Japan and China, and 10-second data from Norway. A few 1-minute data sets were also added to have a little more spatial spread. However, since the conversion to E field involves the time derivative of the magnetic field, and a minute is about the rise time for sudden impulses, the 1-minute data was not desirable. Magnetometer data was downloaded and processed. Initial results provided several points of insight:

1. While not optimal, 1-minute data can be useful if faster cadence data is not available (determined from comparing results for one site that had both 1-minute and 10-second data).
2. Although it may be common to look at geomagnetic disturbances as only one term, the magnitude of the horizontal field, the full vector aspect of the horizontal field should be used.
3. Except for high latitude sites, the rest of the sites did not show strong amplitude variation – little latitude or longitude variation in the disturbance peak.

4. There was one exception to this, however: a site in Brazil had a few peaks that were higher than for other sites, and those high peaks occurred when the site was in mid-day local time.

Recognizing that 1-minute sites were not ideal, but much more readily available, many more sites were added to the evaluation, in order to further confirm the results, and especially to investigate the odd Brazil results. Also, a study was undertaken to try to relate the SI strength to satellite measurements of the solar emission.

### 2. Magnetometer Data Set

The final set of sites used is indicated in red on the map in Figure 1. In South America there was the original Brazil site (VSS), and HUA is in Peru and KOU in French Guiana. There were also added sites in North America and Africa – all added because of the unusually high initial results from the VSS site. A list of sudden impulse events was provided by NOAA (Boulder, Colorado), and from this a set of 22 SI events from 1999 to 2005 was selected. Data, as available, was downloaded for most sites from [1], and for TRO and DOB from [2].

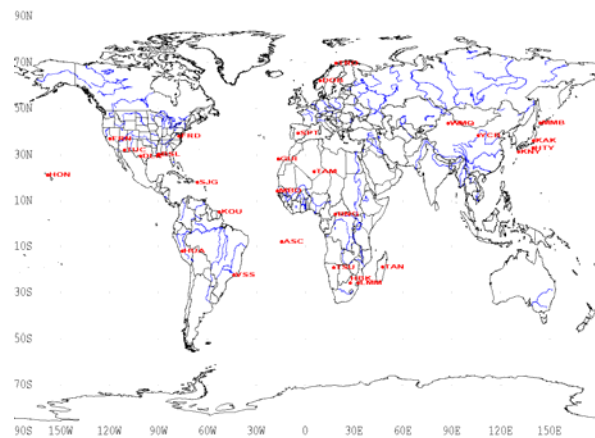


**Figure 1.** Map of the 22 sites used in the sudden impulse study. There are two high latitude sites in Norway, some fast cadence sites in Japan and China, and 1-minute sites in North and South America and Africa.

### 3. B Field Processing and Results

The two vector components of the horizontal B field were separately studied, although for convenience in plots we will show a horizontal magnitude given by

$$B_{XY} = \sqrt{(B_X - B_{X0})^2 + (B_Y - B_{Y0})^2} \quad (1)$$

Here we have removed the magnetic field just before the start of the sudden impulse (subscript “0”). For plots and E field evaluation it is not enough to simply show the disturbance of the magnitude of the horizontal component. For example, declination angle perturbation would be ignored in doing this, yet an angle variation does produce E field disturbance. Assuming that disturbances are only variations in the strength of the quiescent B field is not true.

Figure 2 shows one type of typical result. The Norway sites TRO and DOB develop into very high electrojet disturbances, while the other sites have quick jumps in strength which starts at the time of the “sudden impulse”. We will mostly ignore the high latitude sites TRO and DOB, due to the corruption of the electrojet. The legend lists the sites in general longitude order, west to east, except the four unusual sites have been moved to the end. The numbers in the legend gives the position of the sun relative to each site – the angle from the overhead vertical to the sun divided by  $180^\circ$ , with the sign showing morning (-) or afternoon (+).

The sample in Figure 3 shows that the Norway sites do not always grow into large electrojet disturbances. However, even in this case the signals from these two sites are much different in shape from the other sites. Note also that the highest amplitude is from the HUA (Peru) site. The plot shows that, except for TRO and DOB, the disturbance shapes are very similar for all the sites, and there are not big differences in amplitude, for all sites spread throughout the world. Such correlation of disturbances is not seen for the other types of geomagnetic components.

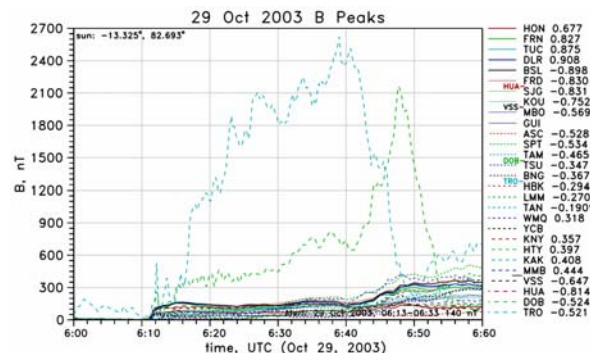


Figure 2. B fields for 6:13 UTC on October 29, 2003. The two large signals are electrojets for the Norway sites.

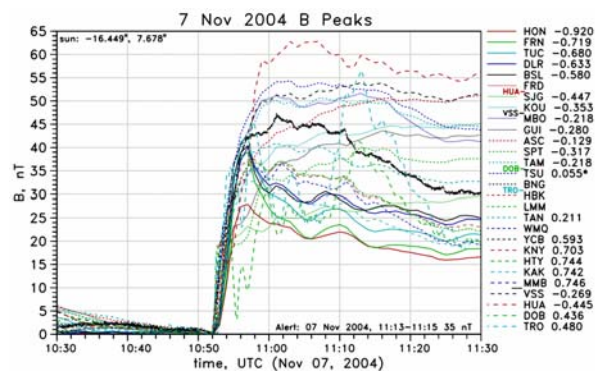


Figure 3. B fields for 11:13 UTC on November 7, 2004.

There is a subtle spatial difference that can be seen among the various sites however. In the following figures the various sites have been separated into two sets for the event in Figure 3. Figure 4 shows sites in which the sudden impulse hits and then the signal tends to gradually grow even higher and stay up at high levels, while in Figure 5 the waveform hits an early peak and then decays in value. In looking at the sun position numbers in the legends we see, generally, that the first set is in the daylight and the second in nighttime. Assuming that the solar emission is hitting on the daylight side, and generating the signal as it compresses the geomagnetic field, then high frequencies (the rise) gets to all places on the Earth, while there is some attenuation of lower frequencies (slow later time part of the signal).

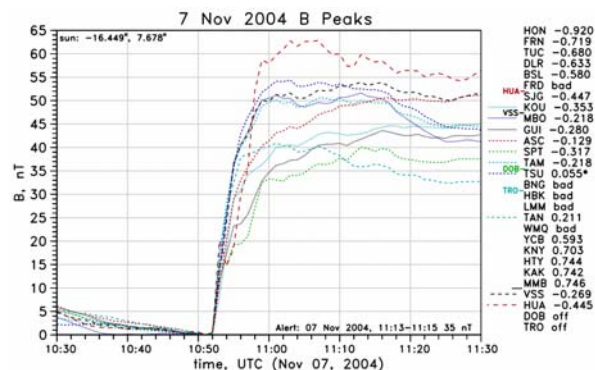


Figure 4. Terms from Figure 3 that stay high.

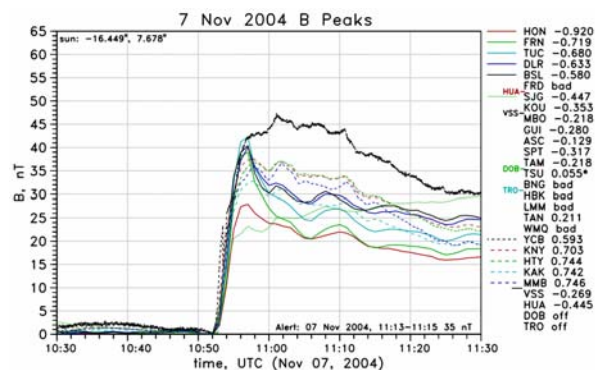


Figure 5. Terms from Figure 3 that decay downward after the peak.

A final example is shown in Figure 6. Here there are three very high signals. Two are the Norway sites which we ignore because of the electrojet. The other is the HUA site in Peru – it is huge compared to the other sites (although still similar in waveshape).

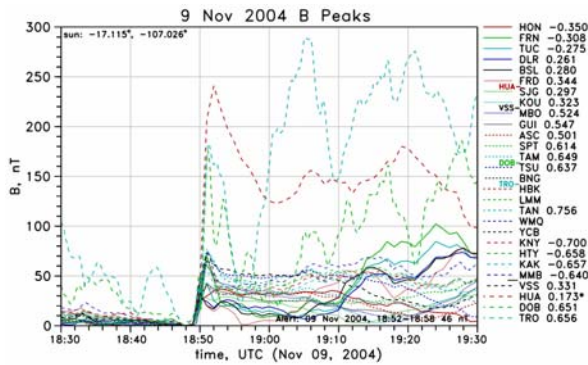


Figure 6. B fields for 18:52 UTC on November 9, 2004.

Peak values were assigned to all the sudden impulse signals (except TRO and DOB). For this we only considered a time window of a few minutes starting at the sudden jump in B field. There is, of course, variations from one geomagnetic storm to another, so all the peak values were normalized by a storm intensity value found from averaging the measurements for all the sites. There is expected to be some noise in this process, such as the arbitrariness in picking the offset values used in Equation 1, however this was done to look for systematic variations.

Figure 7 shows the results for possible dependence of sun exposure angle (the angle has been converted to hours). Points on the left are for the sun directly overhead at the site, while on the right the site is on the opposite point on the Earth (this angle value is related to, but not, the local time). For most of the sites there does not seem to be much solar position dependence, however there is a strong effect for two sites: HUA goes to values 6 times higher if the sun is directly overhead; with the effect falling off at sun angles of about 4 hours; and the effect also affects the VSS site in Brazil (off to the southeast), but to a lesser extent.

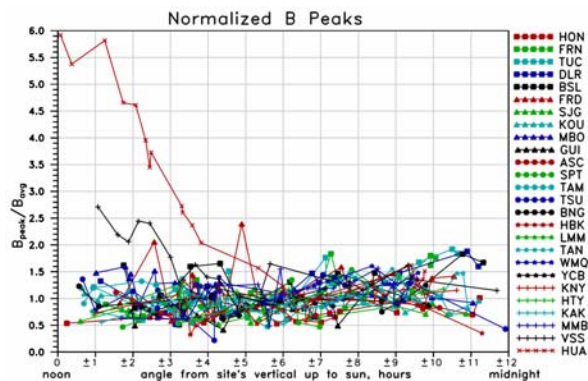


Figure 7. B fields peaks versus local sun position.

Of all the sites, only HUA was very near the geomagnetic equator, and a possible conclusion is that this is an equatorial electrojet effect. The lesser effect at VSS may be due to its proximity to HUS and the equatorial electrojet. However, KOU in French Guiana is also nearby, and there are other sites, such as in Africa, that are closer to the geomagnetic equator than VSS, so the effect is more complicated than just closeness to the geomagnetic equator.

#### 4. Satellite Scaling

ACE (Advanced Composition Explorer) satellite data was used to see if there was a correlation of solar emission particle momentum flux ( $f_p$ , units  $(\#/cm^2) \cdot (km/s)^2$ ) with the sudden impulse strength. Figure 8, for the events for which this data was available, shows the peak B disturbance values normalized by peak values of this storm strength indication. All the data values going into this plot is noisy, however it does appear that an estimate of a SI peak is:

$$B_{\text{peak}} = 5.5 \times 10^{-6} \times f_{p\text{-peak}} \quad (2)$$

Using this conversion, Figure 9 shows a prediction of the B disturbance calculated from the time waveform of the satellite  $f_p$  value for a sample event.

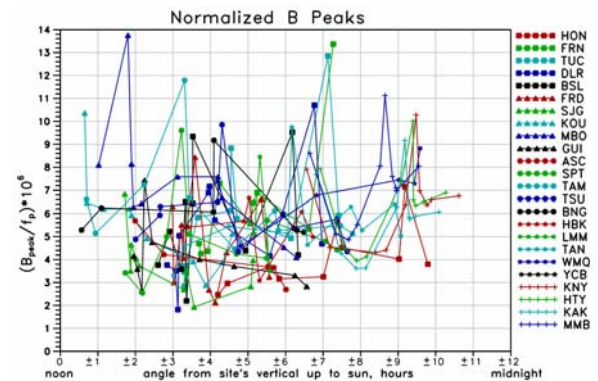


Figure 8. B field peaks normalized by  $f_p$  (without the VSS, HUA, TRO, and DOB unusual sites).

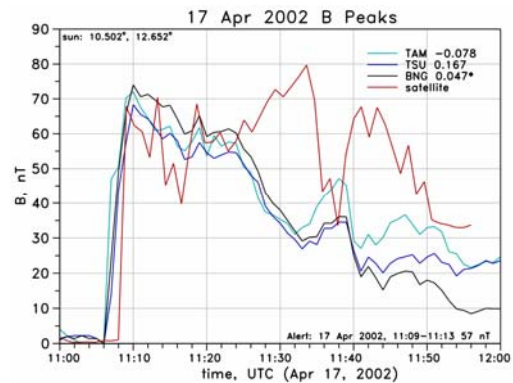
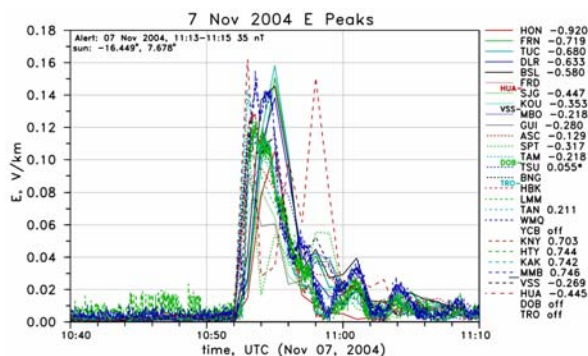


Figure 9. B fields for 11:13 UTC on April 17, 2002. The red line is from Equation 2 applied to the  $f_p$  waveform at the satellite.

## 5. E Field Processing and Results

The conversion to horizontal E field is essentially a complex frequency transfer function that is location dependent, and depends on the ground's composition to deep depths because of the low frequencies of geomagnetic storms (although our implementation is in the time domain [3]). The transfer function is zero at DC, and the algorithm can be set to use the time derivative of the magnetic field (B-dot) to generate the E field, although the E field is not directly proportional to B-dot.

Figure 10 shows the E field for the example B fields in Figure 3. (The time window is only half an hour instead of the full hour in the B plot, the YCB signal was removed because it was so noisy, and the Norway sites are not included.) We see that the signal is dominated by the initial rise of the sudden impulse, and that the various sites are very similar.



**Figure 10.** E fields for 11:13 UTC on November 7, 2004 (the B fields are in Figure 3).

## 6. Signal Rotation

Figure 11 shows the horizontal B field vector behavior for an hour for another example. The time points start at the 0,0 position, and the sudden impulse sends the signal up to the northwest, and then it rolls to the east and then south. This is the initial part of the sudden impulse, the rest of the time the signal randomly wanders off towards the southeast. The important message here is that there is significant rotation here – the signal is not just linear, aligned with the quiescent B field direction. An analysis would miss a substantial part of the signal if it only used the magnitude of the horizontal B field. The corresponding E field is shown in Figure 12. It is even more obvious here that the full vector nature of the disturbance needs to be included. The big loop is from the beginning of the sudden impulse, where the B field first jumps.

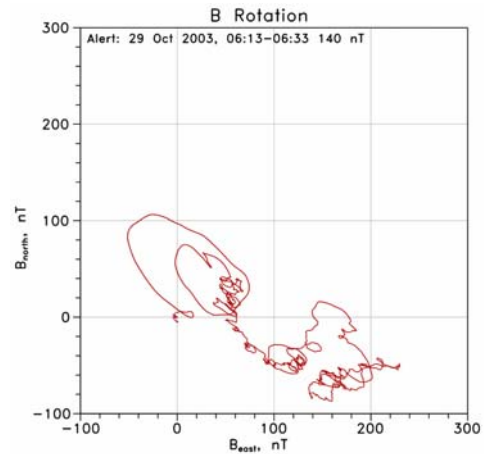


**Figure 11.** Rotation plot of the B field disturbance for the MMB site for the 6:13 October 29, 2003 event.

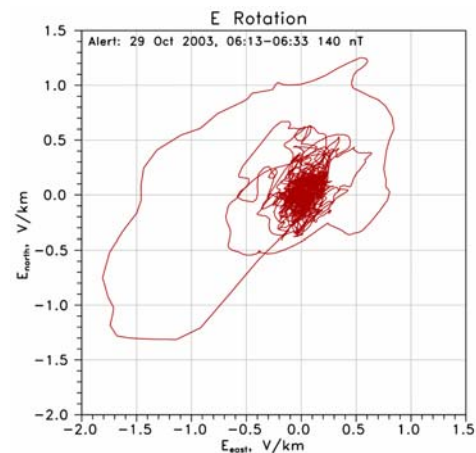


**Figure 11.** Rotation plot of the E field disturbance for the MMB site for the 6:13 October 29, 2003 event.

## 7. References

1. We thank Magnar G. Johnsen at Tromso Geophysical Observatory of UiT The Arctic University of Norway for providing the magnetometer data for stations TRO and DOB.
2. <http://wdc.kugi.kyoto-u.ac.jp/caplot/index.html>
3. J. L. Gilbert, W.A. Radasky, E. B. Savage, "A technique for calculating the currents induced by geomagnetic storms on large high voltage power grids," 2012 IEEE International Symposium on EMC, Pittsburgh, August 2012.